NATIONAL ADVISORY COMMITTEE
FOR AERONAUTICS

REPORT 929

DISLOCATION THEORY OF THE FATIGUE OF METALS

By E. S. MACHLIN

1949

AERONAUTIC SYMBOLS

1. FUNDAMENTAL AND DERIVED UNITS

	Symbol	Metric		English	
		Unit	Abbreviation	Unit	Abbreviation
Length_____	l	meter_____	m	foot (or mile)_____	ft (or mi)
Time_____	t	second_____	s	second (or hour)_____	sec (or hr)
Force_____	F	weight of 1 kilogram_____	kg	weight of 1 pound_____	lb
Power_____	P	horsepower (metric)_____	_____	horsepower_____	hp
Speed_____	V	{ kilometers per hour_____	kph	miles per hour_____	mph
		{ meters per second_____	mps	feet per second_____	fps

2. GENERAL SYMBOLS

W Weight$=mg$

g Standard acceleration of gravity$=9.80665$ m/s^2 or 32.1740 ft/sec^2

m Mass$=\dfrac{W}{g}$

I Moment of inertia$=mk^2$. (Indicate axis of radius of gyration k by proper subscript.)

μ Coefficient of viscosity

ν Kinematic viscosity

ρ Density (mass per unit volume)

Standard density of dry air, 0.12497 kg-m^{-4}-s^2 at 15° C and 760 mm; or 0.002378 lb-ft^{-4} sec^2

Specific weight of "standard" air, 1.2255 kg/m^3 or 0.07651 lb/cu ft

3. AERODYNAMIC SYMBOLS

S Area

S_w Area of wing

G Gap

b Span

c Chord

A Aspect ratio, $\dfrac{b^2}{S}$

V True air speed

q Dynamic pressure, $\dfrac{1}{2}\rho V^2$

L Lift, absolute coefficient $C_L=\dfrac{L}{qS}$

D Drag, absolute coefficient $C_D=\dfrac{D}{qS}$

D_0 Profile drag, absolute coefficient $C_{D_0}=\dfrac{D_0}{qS}$

D_i Induced drag, absolute coefficient $C_{D_i}=\dfrac{D_i}{qS}$

D_p Parasite drag, absolute coefficient $C_{D_p}=\dfrac{D_p}{qS}$

C Cross-wind force, absolute coefficient $C_C=\dfrac{C}{qS}$

i_w Angle of setting of wings (relative to thrust line)

i_t Angle of stabilizer setting (relative to thrust line)

Q Resultant moment

Ω Resultant angular velocity

R Reynolds number, $\rho\dfrac{Vl}{\mu}$ where l is a linear dimension (e.g., for an airfoil of 1.0 ft chord, 100 mph, standard pressure at 15° C, the corresponding Reynolds number is 935,400; or for an airfoil of 1.0 m chord, 100 mps, the corresponding Reynolds number is 6,865,000)

α Angle of attack

ϵ Angle of downwash

α_0 Angle of attack, infinite aspect ratio

α_i Angle of attack, induced

α_a Angle of attack, absolute (measured from zero-lift position)

γ Flight-path angle

REPORT 929

DISLOCATION THEORY OF THE FATIGUE OF METALS

By E. S. MACHLIN

Flight Propulsion Research Laboratory
Cleveland, Ohio

National Advisory Committee for Aeronautics

Headquarters, 1724 F Street NW., Washington 25, D. C.

Created by act of Congress approved March 3, 1915, for the supervision and direction of the scientific study of the problems of flight (U. S. Code, title 50, sec. 151). Its membership was increased from 12 to 15 by act approved March 2, 1929, and to 17 by act approved May 25, 1948. The members are appointed by the President, and serve as such without compensation.

JEROME C. HUNSAKER, Sc. D., Cambridge, Mass., *Chairman*

ALEXANDER WETMORE, Sc. D., Secretary, Smithsonian Institute, *Vice Chairman*

HON. JOHN R. ALISON, Assistant Secretary of Commerce.

DETLEV W. BRONK, PH. D., President, Johns Hopkins University.

KARL T. COMPTON, PH. D., Chairman, Research and Development Board, Department of Defense.

EDWARD U. CONDON, PH. D., Director, National Bureau of Standards.

JAMES H. DOOLITTLE, Sc. D., Vice President, Shell Union Oil Corp.

R. M. HAZEN, B. S., Director of Engineering, Allison Division, General Motors Corp.

WILLIAM LITTLEWOOD, M. E., Vice President, Engineering, American Airlines, Inc.

THEODORE C. LONNQUEST, Rear Admiral, United States Navy, Deputy and Assistant Chief of the Bureau of Aeronautics.

DONALD L. PUTT, Major General, United States Air Force, Director of Research and Development, Office of the Chief of Staff, Matériel.

JOHN D. PRICE, Vice Admiral, United States Navy, Vice Chief of Naval Operations.

ARTHUR E. RAYMOND, Sc. D., Vice President, Engineering, Douglas Aircraft Co., Inc.

FRANCIS W. REICHELDERFER, Sc. D., Chief, United States Weather Bureau.

HON. DELOS W. RENTZEL, Administrator of Civil Aeronautics, Department of Commerce.

HOYT S. VANDENBERG, General, Chief of Staff, United States Air Force.

THEODORE P. WRIGHT, Sc. D., Vice President for Research, Cornell University.

HUGH L. DRYDEN, PH. D., *Director*

JOHN W. CROWLEY, JR., B. S., *Associate Director for Research*

JOHN F. VICTORY, LL.M., *Executive Secretary*

E. H. CHAMBERLIN, *Executive Officer*

HENRY J. E. REID, D. Eng., Director, Langley Aeronautical Laboratory, Langley Field, Va.

SMITH J. DEFRANCE, B. S., Director, Ames Aeronautical Laboratory, Moffett Field, Calif.

EDWARD R. SHARP, Sc. D., Director, Lewis Flight Propulsion Laboratory, Cleveland Airport, Cleveland, Ohio

---

TECHNICAL COMMITTEES

AERODYNAMICS

POWER PLANTS FOR AIRCRAFT

AIRCRAFT CONSTRUCTION

OPERATING PROBLEMS

INDUSTRY CONSULTING

Coordination of Research Needs of Military and Civil Aviation

Preparation of Research Programs

Allocation of Problems

Prevention of Duplication

Consideration of Inventions

LANGLEY AERONAUTICAL LABORATORY, Langley Field, Va.

LEWIS FLIGHT PROPULSION LABORATORY, Cleveland Airport, Cleveland, Ohio

AMES AERONAUTICAL LABORATORY, Moffett Field, Calif.

Conduct, under unified control, for all agencies, of scientific research on the fundamental problems of flight

---

OFFICE OF AERONAUTICAL INTELLIGENCE
Washington, D. C.

Collection, classification, compilation, and dissemination of scientific and technical information on aeronautics

REPORT 929

DISLOCATION THEORY OF THE FATIGUE OF METALS

By E. S. MACHLIN

SUMMARY

A dislocation theory of fatigue failure for annealed solid solutions is presented. On the basis of this theory, an equation giving the dependence of the number of cycles for failure on the stress, the temperature, the material parameters, and the frequency is derived for uniformly stressed specimens. The equation is in quantitative agreement with the data. Inasmuch as one material parameter is indicated to be temperature-dependent and its temperature dependence is unknown, it is impossible to predict the temperature dependence of the number of cycles for failure. A predicted quantitative correlation between fatigue and creep was found to exist, which suggests the practical possibility of obtaining fatigue data for annealed solid solutions and elements from steady-state creep-rate data for these materials. As a result of this investigation, a modification of the equation for the steady-state creep rate previously developed on the basis of the dislocation theory is suggested. Additional data are required to verify completely the dislocation theory of fatigue.

INTRODUCTION

The failure of materials under an oscillating stress, the maximum value of which is lower than that required to cause failure in a static tensile test, is termed "fatigue failure." This type of failure is the limiting factor in the design and the operation of many rotating parts. In particular, fatigue strength has become a limiting factor in the development of the gas turbine for aircraft use. Turbine blades, for example, have in many cases failed as a result of fatigue.

Two methods of eliminating the problem of fatigue failure exist: (1) The design of the parts can be changed to minimize the effect of oscillating stresses; and (2) the resistance to fatigue failure of the materials used can be increased. A phase of the second solution, based on obtaining an understanding of the fatigue phenomena, is discussed herein.

Although many experimental investigations of fatigue have been made, few have been concerned with basic considerations. The work of Gough and his collaborators (references 1 and 2), however, is outstanding in the field of fundamental fatigue studies. This work has shown that the phenomena of plastic deformation (slip) and fatigue are closely related. Some theories have been reported (references 3 and 4) that relate plastic deformation to fatigue failure. Because these theories are not of a fundamental nature, however, they have not yielded basic knowledge of the physical properties of materials that affect fatigue.

With the development of the theory of dislocations, the understanding of the phenomena of plastic deformation has greatly advanced (references 5 to 8). Inasmuch as plastic deformation and fatigue have been shown to be related, an investigation of fatigue based on the theory of dislocations was undertaken during 1947 and is presented herein. In this investigation a physical model, based on the dislocation theory, was devised to account for crack growth. This model was then used as a means of obtaining an equation relating the number of cycles for failure to the appropriate variables. The equation so obtained was then subjected to various experimental checks. This investigation was part of a program conducted at the NACA Cleveland laboratory to evaluate the physical properties of heat-resisting alloys in terms of physical constants that are easily measurable and to make possible the synthesis of compositions and structures of heat-resisting alloys better than those currently used.

SYMBOLS

The following symbols are used in this report:

a	constant
c	proportionality constant relating τ_a to $\sigma_m/2$
d_1	distance between atoms in slip direction, centimeters
exp	base of Napierian logarithmic system raised to power in parentheses following exp
f	fraction, experimental value$=0.374$ (reference 8)
ΔF_g	free energy of activation involved in generation of a dislocation, ergs per molecule
h	Planck's constant, 6.62×10^{-27} erg seconds
ΔH_g	heat of activation per molecule involved in generation of a dislocation, ergs
k	Boltzmann's constant, 1.38×10^{-16} ergs per molecule per °K
L	distance between imperfections in single crystal, of order of 1 micron
M	amount of crack growth per crack source necessary for failure measured in units of number of interatomic spacings
N	number of cycles for failure
P	period of cycle of stress, seconds
q	stress-concentration factor
q'	cq
R_d	rate of generation of positive or negative dislocations at stress concentration of internal surface in crystalline material, number of dislocations per second
R_g	net rate of growth per crack, number of atomic spacings per second

ΔS_g entropy of activation per molecule involved in generation of dislocation, ergs per °K

T absolute temperature, °K

t time, seconds

u' shear rate, 1 per second

u_i antilog of intercept of plot of log u' against σ at $\sigma=0$

V atomic volume, cubic centimeters

x ratio of d_1 to interplanar spacing of slip planes, ($\sqrt{3/2}$ for face-centered and body-centered cubic lattices)

y mathematical variable

θ $2\pi\omega t$

σ tensile stress, dynes per square centimeter

σ_m maximum tensile or compressive stress of cycle, dynes per square centimeter

τ resolved shear stress, dynes per square centimeter

τ_a average resolved shear stress in polycrystalline specimen operating for failure, dynes per square centimeter

τ_i resolved shear stress due to internal source, dynes per square centimeter

τ_m resolved maximum shear stress corresponding to σ_m, dynes per square centimeter

τ_s average shear stress at sources of dislocations, dynes per square centimeter

ω frequency of cycles of stress application, 1 per second

CRACK MECHANISM

Fatigue failure is usually associated with the propagation of a crack. This fatigue crack must be formed either as a result of internal tensile stresses that exceed the tensile strength of the material or from pre-existing submicroscopic cracks that grow under the influence of the cyclic stress. The assumption will be made that such submicroscopic cracks do exist. It is probable that some of the sources of stress concentrations in metals are in the form of submicroscopic cracks that occur at the boundaries of mosaic blocks (reference 6).

A theory that would explain the growth of these submicroscopic cracks as a result of the continual reversal of stress might provide a basis for the development of a quantitative theory of fatigue. The analysis of the mechanism of crack formation developed herein is based on the dislocation theory discussed in references 5, 6, 8, and 9. A short résumé of the dislocation theory follows:

A dislocation consists of a stable arrangement of atoms such that, in a region of a few atomic distances, $n+1$ atoms in the slip direction face n atoms across the slip plane. When the $n+1$ atoms are above the n atoms, the configuration is called a positive dislocation; when the $n+1$ atoms are below, it is called a negative dislocation. The net result of a positive dislocation moving completely through a specimen from left to right, or a negative dislocation moving completely through the specimen from right to left, is a translation of the material above the plane between the $n+1$ atoms and the n atoms, with respect to the material below this plane, by

one atomic distance to the right. If the positive dislocation moves from right to left or the negative dislocation moves from left to right, the opposite translation takes place.
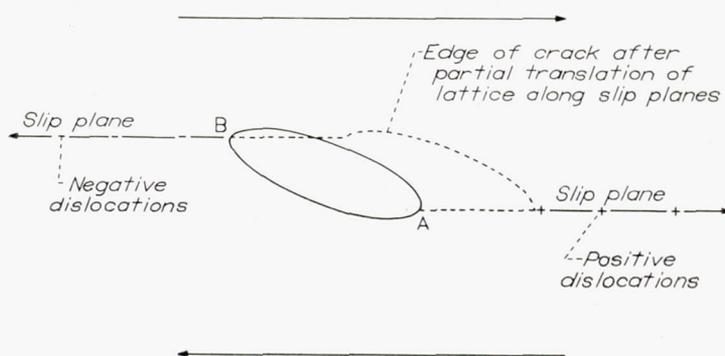
FIGURE 1.—Single crack generating source of dislocations.

The most probable sources of generation of dislocations are stress concentrations. Such stress concentrations occur at the ends of cracks. For example, an ellipsoidal crack shown in cross section in figure 1, has two points of stress concentration (A and B in fig. 1), that exceed the stress concentration at any other point along the crack circumference (reference 10). Dislocations will usually be generated at these stress concentrations upon the application of a shear stress.

In the development of a theory for the growth of submicroscopic cracks, an equation that was in agreement with the available data was obtained by making certain assumptions about the physical model. Although each of these assumptions may have a physical basis, such a basis was not immediately evident. The development of the following theory therefore presents these assumptions without any attempt to justify them physically.

Cracks similar to the one diagrammatically shown in figure 1 are assumed to exist in such a manner that points A and B act as sources of generation of dislocations. It is further assumed that only positive dislocations can be generated at point A and only negative dislocations can be generated at point B. If the line joining A and B is at a small angle to the slip plane, if the generated positive dislocations move to the right at point A and if the generated negative dislocations move to the left at point B as a result of the given shear stress, the crack will grow. An intermediate position of the right side of the crack after the crack has grown to some extent is shown by the dashed line in figure 1.

If all the dislocations that were generated at A and B during one half-cycle of stress had returned to their respective sources during the next half-cycle of stress, the crack would not have grown at the end of a complete cycle of reversed stressing. In order for the crack to grow, some of the dislocations generated at the crack sources during the growth part of the stress cycle therefore must either disappear from the specimen or reach a point from which their return to the source is prevented. No dislocations generated at A and B in the second half-cycle of stress can enter the crystal

lattice because, according to the assumption, only positive dislocations are generated at A, only negative dislocations are generated at B, and the applied stress during this half-cycle of stress would make any dislocations generated at these sources return to their respective sources. This assumption does not mean, however, that other sources, at which none of the dislocations there generated move into the crystal lattice during the first half-cycle, will not generate dislocations that move into the crystal lattice in the last half-cycle.

If one submicroscopic crack were to account for the failure of a macroscopic specimen, it is probable that more than the observed amount of plastic flow would have to occur. If failure were to occur as the result of the growth of submicroscopic cracks, it would evidently take place because many cracks contribute to the failure. A simple configuration of cracks of the type illustrated in figure 1 that can lead to fatigue failure with little plastic flow is shown in figure 2(a).
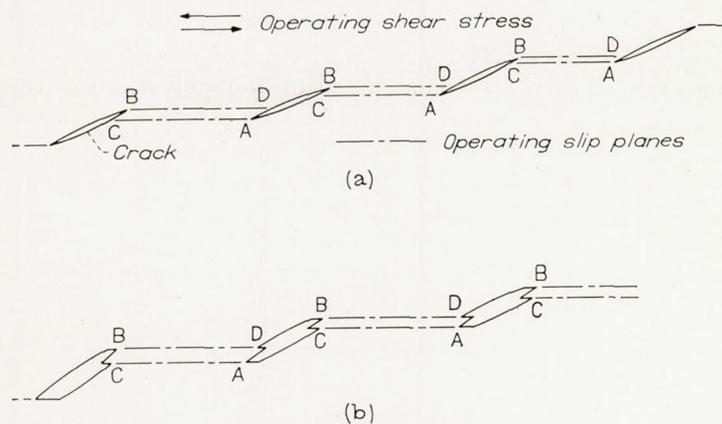
(a) Leading to fatigue failure.
(b) Leading to growth of cracks after partial slip has occurred.

FIGURE 2.—Submicroscopic-crack configuration.

This configuration, after all the cracks have grown to a certain extent, would appear as shown in figure 2(b). In order that the cracks in this configuration may grow, the assumption becomes necessary, as before, that at points A only positive dislocations are generated and at points B only negative dislocations are generated. The result of positive dislocations moving to the left and negative dislocations simultaneously moving to the right during a cycle of stress favorable for this motion is that relative translations of the lattice occur that yield larger cracks than existed prior to the translations. Inasmuch as these dislocations disappeared from the lattice at points C and D in figure 2(a), the application of a stress opposite to the previous stress would not cause any relative translations of the lattice between the regions separated by the slip planes A–C and B–D, unless positive and negative dislocations were generated at C and D, respectively. No dislocations are assumed to be generated at points C and D. Each crack in the configuration will therefore grow as long as positive dislocations generated at A

and negative dislocations generated at B disappear from the lattice at C and D, respectively.

In the foregoing discussion, each crack was assumed to extend completely through the specimen in the direction perpendicular to the plane of the figure. Because the cracks were assumed to exist in the mosaic-block boundaries, it seems probable, however, that the crack width in the direction considered is not more than a few mosaic-block lengths, that is, about 10^{-4} centimeters. In order to account for the growth of short cracks, it thus becomes necessary to assume that such short dislocations may exist and that relative slip between mosaic blocks may easily occur. Seitz and Read in considering the phenomena of slip with respect to dislocations found that these assumptions would help explain the experimental slip phenomena (reference 6, pt. II).

One of the consequences of the crack-growth mechanism just described is that the cracks will begin to grow along slip planes. This phenomenon has been observed by a number of experimenters (for example, references 2 and 11) on polycrystalline as well as single-crystal specimens. It was noticed that failure began to occur along the slip plane and then proceeded in the direction normal to the maximum tensile stress.

NUMBER OF CYCLES FOR FAILURE

The general equation for the rate of generation of dislocations R_d of one type at a stress concentration of an internal surface in a crystalline material is given in reference 8. The equation, for large values of $\frac{2qVxf\tau}{kT}$, can be written as

$$R_d = \frac{kT}{h} \, exp \left(\frac{-\Delta F_g}{kT} + \frac{2qVxf\tau}{kT} \right) \qquad (1)$$

The net rate of growth per crack R_g is the rate of generation of dislocations during the growth cycle:

$$R_g = R_d = \frac{kT}{h} \, exp \left(\frac{-\Delta F_g}{kT} + \frac{2qVxf\tau}{kT} \right) \qquad (2)$$

The stress at a generating source may consist of the applied stress and any internal stress that may be present. As a result,

$$\tau_s = q\tau = q(\tau_m \sin \theta + \tau_i) \qquad (3)$$

If it is assumed that the amount of crack growth per crack source required for failure M is a constant for all specimens and materials and that the stress-concentration values are the same for every crack associated with failure and do not change with the number of cycles of stressing, the dependence of the number of cycles for failure on the maximum resolved shear stress in the slip plane and direction considered is

$$M = N \int_0^{\frac{P}{2}} R_g \, dt \qquad (4)$$

because R_g is independent of N. Substituting for R_g in equation (4) yields

$$M = N \frac{kT}{h} \left[exp \left(\frac{-\Delta F_g}{kT} \right) \right] \int_0^{\frac{P}{2}} exp \left(\frac{2qVxf\tau}{kT} \right) dt \qquad (5)$$

For annealed metals, the internal stress τ_i is approximately zero. Thus,

$$\tau = \tau_m \sin \theta$$

Changing the variable of integration in equation (5) yields

$$M = \frac{NkT}{2\pi\omega h} \left[exp \left(\frac{-\Delta F_g}{kT} \right) \right] \int_0^{\pi} exp \left(\frac{2qVxf\tau_m \sin \theta}{kT} \right) d\theta \qquad (6)$$

The expression $\log_e \int_0^{\pi} exp \, (ay \sin \theta) \, d\theta$ can be approximated for large values of ay, by the product ay, as shown in appendix A. When this approximation is used in equation (6) and equation (6) is solved for $\log N$

$$\log N \cong \log \left(\frac{2\pi\omega h M}{kT} \right) + \frac{\Delta F_g}{2.3kT} - \frac{2qVxf\tau_m}{2.3kT} \qquad (7)$$

In order to apply equation (7) to polycrystalline specimens, some assumptions must be made concerning the method of fatigue failure of polycrystals. The orientations of the crystals comprising the fatigue-failed regions of a polycrystal are probably random. The maximum resolved maximum shear stress, if each of these crystals was considered apart from the others, would therefore vary from some minimum (not zero for face-centered cubic or body-centered cubic lattices) to the maximum $\sigma_m/2$. Inasmuch as these crystals are not separated by stress-free regions, internal stresses would be set up between the differently oriented crystals. As a result, steady-state slip would occur at some stress intermediate to the minimum and maximum value of the maximum resolved maximum shear stress. The value of this average resolved shear stress should then be substituted in equation (7) for polycrystalline specimens. If the average resolved shear stress is related to the maximum resolved shear stress by the equation $\tau_a = c \frac{\sigma_m}{2}$ and if $q' = cq$, then,

$$\log N = \log \left(\frac{2\pi\omega h M}{kT} \right) + \frac{\Delta F_g}{2.3kT} - \frac{q'Vxf\sigma_m}{2.3kT} \qquad (8)$$

Equation (8) applies only for stresses sufficiently above the endurance limit (where the $\log N$ varies linearly with σ_m) because the conditions that determine the endurance limit have not been considered in the development of the theory. Also, because the assumption was made that σ_m is constant over the cross section of the specimen, equation (8) will apply to axial-stress-type loading only. The cases of bending-type stresses and torsional stresses are theoretically capable of being treated in a manner similar to the case of uniform axial stress; however, no attempt has been made to evaluate equations of the same type as equation (8) for these cases.

According to equation (8), the intercept of the straight line obtained by plotting $\log N$ against σ_m at $\sigma_m = 0$ is equal to

$$\log \left(\frac{2\pi\omega h M}{kT} \right) + \frac{\Delta F_g}{2.3kT}$$

If all the parameters in this expression are known, it should be possible to obtain a calculated value of the intercept to compare with the experimental value. The parameters ω and T are known from the experimental conditions. The parameter M is of the order of magnitude of a mosaic block length, measured in units of interatomic spacings, that is, about 10^4. The parameters k and h are known constants. The only factor that remains to be determined is ΔF_g. A method of calculating ΔF_g by using creep data is presented in reference 8. As shown in appendix B, however, ΔF_g cannot be completely determined from creep data because an assumption made in reference 8 is incorrect. The analysis presented in appendix B does indicate, however, that a set of fatigue and creep data for the same material can be used to calculate a value of the unknown factor. If the value of this factor is assumed to be independent of the material variable, it can be used to help calculate values of ΔF_g using creep data. A table of such calculated values using data for copper (fig. 3(a)) to evaluate the unknown factor is presented in appendix B.

(a) Copper.
(b) Armco iron.
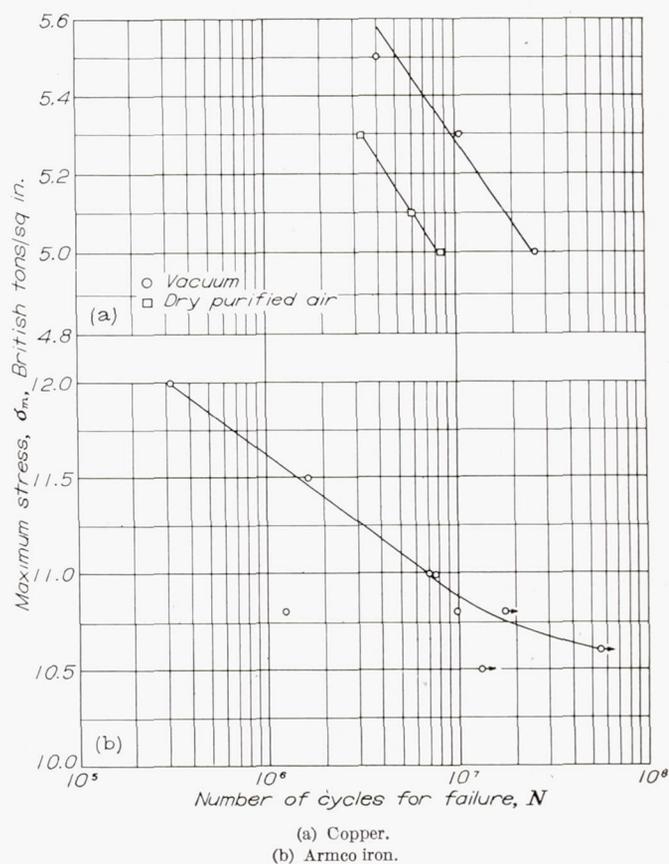
FIGURE 3.—Variation of stress with number of cycles for failure at room temperature. Frequency, 2200 cycles per minute. (Data taken from reference 12.)

A check of equation (8) can be made by comparing the experimental value of the intercept of the straight line obtained by plotting $\log N$ against σ_m with the value obtained from calculation using the term derived from equation (8). Data for Armco iron, obtained from reference 12 and plotted in figure 3(b), can be used to make the suggested comparison of experimental and calculated values of the intercept being considered. The experimental value of the intercept determined by extrapolating the best straight line through the points of figure 3(b) is equal to 22. The approximate uncertainty in this value is ±2. The calculated value is

$$\log\left(\frac{2\pi\omega h M}{kT}\right)+\frac{\Delta F_g}{2.3kT}=\log\left(\frac{2\pi\times\dfrac{2200}{60}\times6.62\times10^{-27}\times10^4}{1.38\times10^{-16}\times300}\right)+$$

$$\frac{2.92\times10^{-12}}{2.3\times1.38\times10^{-16}\times300}=24.2$$

where $\omega=2200$ cycles per minute and $T=300°$ K, as given by reference 12. The agreement between the predicted value of 24.2 and the observed value of 22 ± 2 tends to verify equation (8).

An additional check of the validity of equation (8) could be made if the value of the stress-concentration factor q were known. Because the value of q is unknown, the experimental value of the slope of the linear portion of the plot of $\log N$ against σ_m can be used to obtain a value of q'. This calculation is

$$q'=\frac{2.3\,kT\times(\text{experimental slope, sq cm/dynes})}{V\times x\times f}$$

$$=\frac{2.3\times1.38\times300\times10^{-16}\left(\dfrac{1}{0.755\times2240\times6.9\times10^4}\right)}{11.7\times10^{-24}\times1.23\times0.374}$$

$$=152$$

A similar procedure was followed to obtain a value of q' for annealed copper using the line shown in figure 3(a) to define the slope. A value of $q'=164$ was obtained.

The fatigue theory can be further experimentally checked. If equation (8) is solved for the parameter $V\sigma_m$, the following equation is obtained:

$$V\sigma_m=U+W\Delta F_g \tag{9}$$

where

$$U=\left(\frac{2.3\,kT}{q'xf}\right)\left[\log\left(\frac{2\pi\omega h M}{kT}\right)-\log N\right]$$

$$W=\frac{1}{q'xf}$$

Data to check equation (9) were obtained from a number of sources. The details concerning the sources and precision of data for ΔF_g are contained in appendix B.

Because the data for the value of σ_m that corresponds to failure in 3.3×10^6 cycles were difficult to obtain accurately, the following table lists, wherever possible, a number of sources for a given material:

Material	σ_m, dynes/sq cm	Reference
Aluminum	3.5×10^8	13
Silver[a]	6.2	14
Copper	8.2	12
	8.65	15
Armco iron	1.74×10^9	12
	1.90	16
Nickel	2.06	17
	2.98	15

[a]Data obtained from experiment applying torsional stresses to a single crystal. Because the corrections involved are in opposite directions, the value given is a fair approximation.

Inasmuch as different sources yielded different values of the stress corresponding to a certain number of cycles for failure for a given material and because the values of ΔF_g were obtained by extrapolation, the data were plotted as regions of approximately equal probability corresponding to each material. The data are therefore plotted as rectangles or lines in figure 4. The data in this figure correspond to
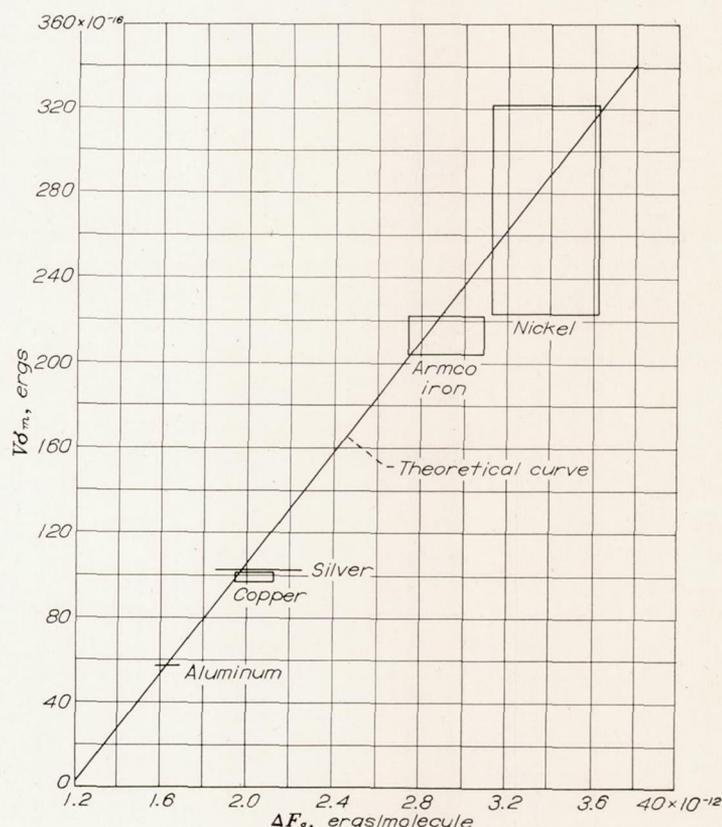
FIGURE 4.—Dependence of stress corresponding to failure in 3.3×10^6 cycles on material parameters at room temperature.

failure in approximately 3.3×10^6 cycles; the frequency used to calculate U is 2200 cycles per minute; the temperature is $300°$ K.

The theoretical curve corresponding to these data is, according to equation (9), a straight line of slope W and intercept U. The value of q' was considered to be 164, as previously found for annealed copper. Because all the other factors involved in the calculation of U and W are known, calculation of the theoretical values of U and W is possible.

The calculated values of U and W are -157×10^{-16} ergs per molecule and 0.0132, respectively. The theoretical curve corresponding to these values of U and W is plotted as the straight line in figure 4; the theoretical line is in agreement with the data. Figure 4 represents a correlation between creep and fatigue, inasmuch as the ordinate is a parameter determined from fatigue data and the abscissa is a parameter determined from creep data.

Two other independent checks of the theory are possible: The first is a check of the temperature dependence of the number of cycles for failure; the second is based on the dependence of the number of cycles for failure on frequency.

The assumption is made that q is independent of temperature. If equation (8) is solved for σ_m, the following equation is obtained:

$$\sigma_m = A + B(C - \log T) T \qquad (10)$$

where

$$A = \frac{\Delta H_g}{q' V x f}$$

$$B = \frac{2.3k}{q' V x f}$$

$$C = \log \left(\frac{2\pi \omega h M}{k N} \right) - \frac{\Delta S_g}{2.3k}$$

Data for Armco iron obtained from reference 16 are shown in figure 5. A cross plot of these data (temperatures in °K) is shown in figure 6, which also gives the theoretical curve corresponding to this experimental plot. Data used to compute the theoretical values were obtained as follows: Values of $\Delta H_g / V$ correspond to values of A/V from figure 6 of reference 8; values of ΔS_g were taken from the values listed in the table given on page 16 of reference 8, corrected to account for the factor determined in appendix B; the value of q' was taken as 164; the frequency ω was taken as 40 cycles per second, as reported in reference 16.

A study of figure 6 indicates that the theoretical curve yields too small a temperature variation of σ_m. Therefore, equation (10) apparently does not agree with the experimental data. Two explanations of these results are possible. The first explanation is that the data may be in error. The large scatter for the data corresponding to 500° C, as shown in figure 5, indicates that this explanation may be true. Furthermore, meaningful temperature studies on direct-stress specimens are difficult to perform because the specimen may easily become misalined, owing to the use of long specimen holders. The misalinement may then be a function of temperature and yield an apparent temperature effect, as shown in figure 6.

The second and more probable explanation is that the stress concentrations associated with the cracks in the mosaic-block boundaries are temperature-dependent and, hence, the assumption made in plotting the theoretical curve in figure 6 is not valid. In this case, predicting the temperature dependence of σ_m becomes difficult inasmuch as no apparent basis exists for determining the dependence of the stress-concentration factor on temperature.

A final check of the dislocation theory of fatigue can be obtained by determining whether the dependence of the number of cycles for failure on the frequency, as given by equation (8), is experimentally obtained. Equation (8) also indicates that $\log N$ would be linearly related to $\log \omega$ at constant maximum stress and temperature. The experiments reported in reference 18 yield results that qualitatively

FIGURE 5.—Temperature dependence of curve for σ_m plotted against N for Armco iron. (Data taken from reference 16.)
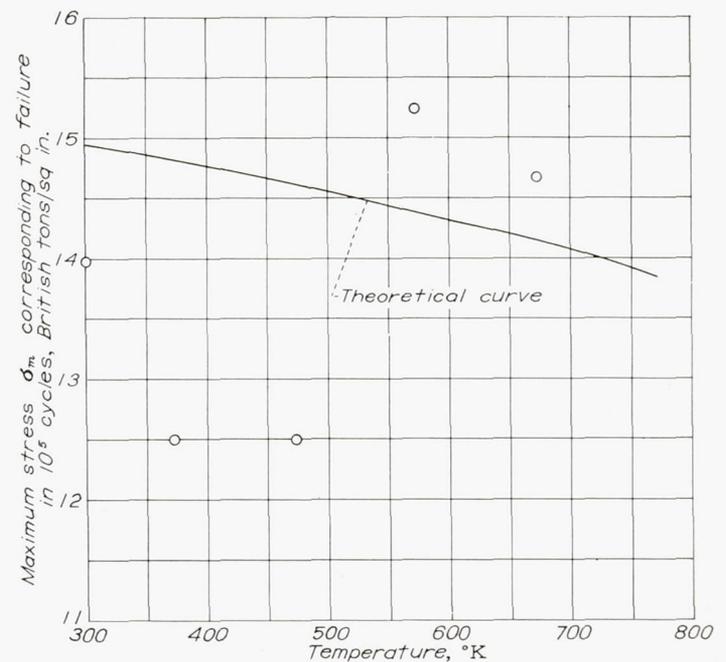
FIGURE 6.—Temperature dependence of stress corresponding to failure in 10^5 cycles for Armco iron.

verify the prediction. In reference 18, direct-stress experiments performed at 7000 cycles per minute required a greater number of cycles for failure than tests at 1200 cycles per minute. The tests at 1200 cycles per minute, however, were performed on a different type machine than the tests at 7000 cycles per minute; therefore, the results would not be expected to agree quantitatively. The increase in log N was nevertheless sufficiently large that it is improbable that the difference in machines could be solely responsible for the effect noticed. Reference 19 indicates that no frequency effect occurs at low values of frequency. An examination of the data, however, reveals that more data would be required in order to be able to draw any conclusion concerning this effect.

EVALUATION OF RESULTS

Sufficient data to verify equation (8) completely are unavailable. Inasmuch as this equation is in quantitative agreement with available data, further experimentation designed to verify the dislocation theory of fatigue is justified.

The theory was developed for annealed elements or solid solutions; the data used to check the theory were obtained only from annealed elements. It seems reasonable, however, that data for annealed solid solutions would also be in agreement with the theory.

It is improbable that equation (8) would apply to the case of precipitation-hardened or strain-hardened materials because certain modifications, such as the introduction of an internal-stress term, would be necessary. This subject is sufficiently complex to justify an independent investigation.

The uncertainty in the data appears sufficiently large to allow reasonable doubt in the constancy of the stress-concentration factor q for all annealed elements and solid solutions. The possibility exists that an experimental plot of $q'V\sigma_m$ against ΔF_g would also be linear; however, the data are insufficient to resolve this question.

The number of cycles for failure at some given stress and temperature have been experimentally observed to follow a statistical distribution (reference 20). An explanation of this phenomenon on the basis of equation (8) would probably require that one or more of the following factors, M, ΔF_g, and q assume a range of values for a given material. It seems reasonable that the factors M and q may vary from specimen to specimen inasmuch as these quantities are probably dependent on manufacturing variables such as casting, drawing, and heat-treating. On the basis of the dislocation theory, accounting for the scatter of data normally obtained in fatigue tests is thus possible.

In figure 4, which helps substantiate equation (8), a correlation between fatigue and creep is established as predicted by the theory and fatigue failure is proved to depend on plastic deformation. With the assumption of a constant value of q at room temperature, the prediction of fatigue data from a knowledge of creep data for annealed elements and solid solutions is made possible for practical purposes.

APPENDIX A

EVALUATION OF DEFINITE INTEGRAL

The definite integral

$$\int_0^\pi exp\ (ay \sin \theta)\ d\theta$$

was evaluated for a series of values of ay by numerical integration. The value of a was set equal to 10.56×10^{-8} to correspond approximately to the expected values of the physical quantity it represented. A plot of the log of the integral against y is shown in figure 7. For values of $y > 10^8$, the equation of the curve is

$$\log \int_0^\pi exp\ (10.56 \times 10^{-8} y \sin \theta)\ d\theta \simeq by$$

where b is the slope of the line in figure 7, 4.44×10^{-8}. As a result,

$$\log_e \int_0^\pi exp\ (10.56 \times 10^{-8} y \sin \theta)\ d\theta \simeq 10.22\ y \times 10^{-8}$$

or

$$\log_e \int_0^\pi exp\ (ay \sin \theta)\ d\theta \simeq ay$$
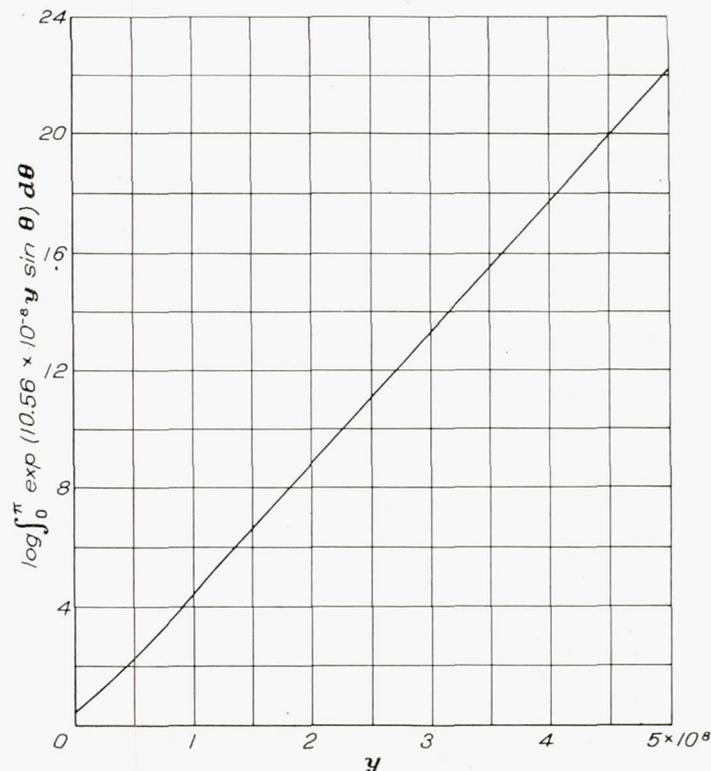
FIGURE 7.—Variation of log $\int_0^\pi exp\ (10.56 \times 10^{-8}\ y \sin \theta)\ d\theta$ with y.

8

APPENDIX B

EVALUATION OF ΔF_g

The equation

$$u' = 10^{-4} \frac{kT}{h} \, exp \left(\frac{-\Delta F_g}{kT} + \frac{2qVxf\tau}{kT} \right)$$

obtained from reference 8 was first used to calculate values of ΔF_g from steady-state creep-rate data. This calculation was accomplished by plotting log u' against σ, setting the experimental value of the intercept at $\sigma = 0$ equal to

$$\left(-4 + \log \frac{kT}{h} - \frac{\Delta F_g}{2.3kT} \right)$$

and solving for ΔF_g because all the other parameters are known in the expression for the intercept. When these values of ΔF_g were used to calculate the intercepts of the curves of log N plotted against σ_m and $V\sigma_m$ plotted against ΔF_g, the calculated intercepts were found to exceed the experimental intercepts by a factor that varied between 1×10^{-13} to 3×10^{-13} ergs per molecule in the value of ΔF_g. In attempting to find an explanation for this discrepancy, an assumption made in reference 8 regarding the value and constancy of the quantity 10^{-4} in the preceding equation was found to be erroneous. The value of 10^{-4} was used as an approximation for d_1/L. In the derivation of the foregoing equation, the value of 10^{-4} was based on an assumption that one source of generation of dislocations exists per mosaic block. Thus, according to this assumption, the strain due to the passage of one dislocation through a mosaic block is $\frac{d_1}{L} \cong \frac{3 \times 10^{-8}}{3 \times 10^{-4}} \cong 10^{-4}$. Evidence exists, however, for single crystals, which indicates that the spacings between slip planes may be many multiples greater than 3×10^{-4}. For example, figure 8, which was taken from reference 21, indicates that the spacing may be as large as 0.3 centimeter and figure 9 indicates that $1/L$ (number of slip planes/cm) may vary between 0 and 7500. Thus, the assumption that L is a constant for polycrystals of magnitude 3×10^{-4} is probably incorrect. It remains to be shown, however, how L may be calculated.

Without a physical model of the mechanism of strain in a polycrystal, it seems that the simplest assumption is to leave the factor d_1/L as an unknown constant 10^C. The factor C can then be determined from a set of fatigue and creep data for the same material as follows: From equation (8), it is evident that the intercept of the straight line obtained by plotting log N against σ_m at $\sigma_m = 0$ is

$$\log \left(\frac{2\pi\omega hM}{kT} \right) + \frac{\Delta F_g}{2.3kT}$$

The data for annealed copper shown in figure 3(a) were used in this calculation. The data for dry purified air were used to locate the slope of the line taken through the points for the determinations in vacuum. The intercept of this line

Temperature
(°C)

FIGURE 8.—Pure aluminum sample elongated at different temperatures by application of stress. Most of plastic flow occurs along slip bands. Not etched. X15. (Taken from fig. 14 of reference 21.)
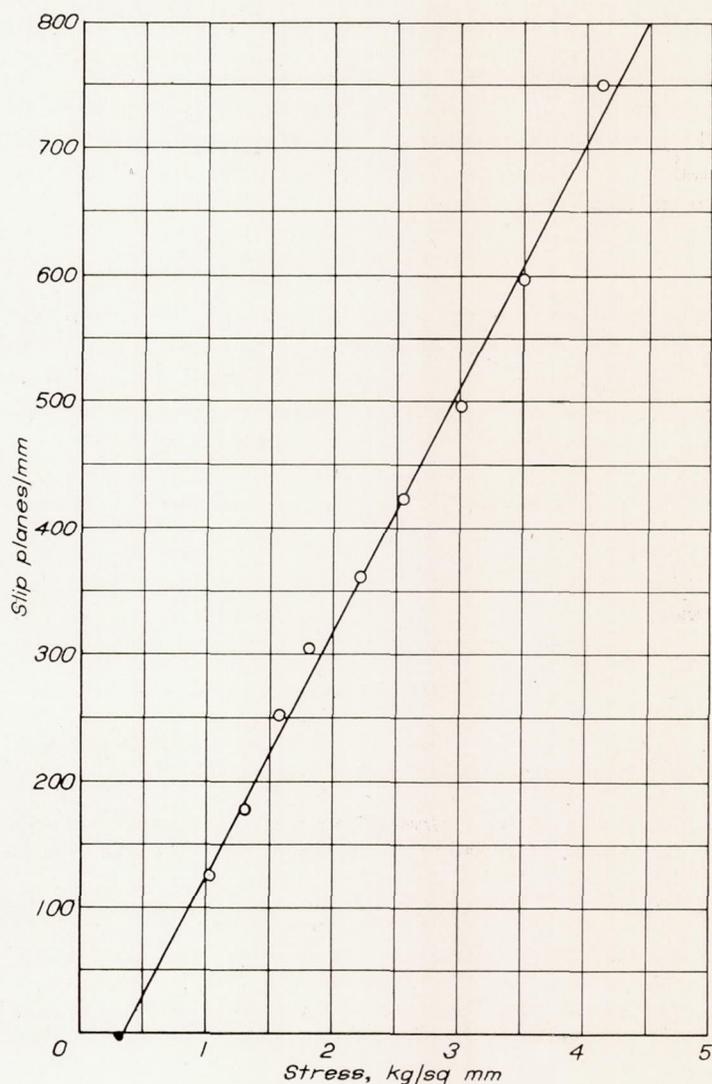
FIGURE 9.—Stress dependence of number of slip planes per millimeter. (Taken from fig. 24 of reference 26.)

9

was found to equal approximately 15. Hence,

$$\Delta F_g = \left[15 - \log \left(\frac{2\pi \times \frac{2200}{60} \times 6.62 \times 10^{-27} \times 10^4}{1.38 \times 10^{-16} \times 300} \right) \right] 2.3 \times 1.38 \times 10^{-16} \times 300$$

$$= 2.01 \times 10^{-12} \text{ ergs/molecule}$$

where $\omega = 2200$ cycles per minute and $T = 300°$ K, as given by reference 12.

From the creep equation,

$$\log u' = C + \log \frac{kT}{h} - \frac{\Delta F_g}{2.3kT} + \frac{2qVxf\tau}{kT}$$

it is apparent that the intercept $\log u_i$ of the straight line obtained by plotting $\log u'$ against τ at $\tau = 0$ is

$$\log u_i = C + \log \frac{kT}{h} - \frac{\Delta F_g}{2.3 kT}$$

An estimate of $\log u_i$ at $300°$ K can be obtained from data given at other temperatures by plotting $\left(T \log \frac{u_i}{T} \right)$ against $\frac{1}{T}$, because ΔF_g is linearly dependent on T, and by extrapolating the best straight line thus obtained to $T = 300°$ K. From the data of references 22 and 23, an average value of -15 was obtained for $\log u_i$. When this value was substituted for $\log u_i$ and $\Delta F_g = 2.01 \times 10^{-12}$ in the preceding equation, solving for C yielded

$$C = -6.7$$

For the purpose of obtaining values of ΔF_g from creep data for other materials, C was assumed to be a constant. When this value of C was used, values of ΔF_g were obtained from creep data and are given in the following table together with a list of the sources of the respective data:

Material	ΔF_g, ergs/molecule	Reference
Aluminum	1.57–1.70×10⁻¹²	21, 24
Silver	1.85–2.26	21
Copper	1.94–2.12	22, 23
Armco iron	2.74–3.09	25
Nickel	3.13–3.63	21

REFERENCES

1. Gough, Herbert John: Fatigue Phenomena, with Special Reference to Single Crystals. Jour. Roy. Soc. Arts, vol. LXXVI, no. 3955, Sept. 7, 1928.
2. Gough, Herbert John: Crystalline Structure in Relation to Failure of Metals—Especially by Fatigue. A. S. T. M., Proc., vol. 33, pt. II, 1933, pp. 3–114.
3. Orowan, E.: Theory of the Fatigue of Metals. Proc. Roy. Soc. (London), ser. A, vol. CLXXI, 1939, pp. 79–106.
4. Afanasev, N. N.: Statistical Theory of the Fatigue of Metals. Jour. Tech. Phys. (U. S. S. R.), vol. 10, 1940, pp. 1553–1568.
5. Taylor, G. I.: The Mechanism of Plastic Deformation of Crystals. I—Theoretical. II—Comparison with Observations. Proc. Roy. Soc. (London), ser. A, vol. CXLV, no. A 855, July 2, 1934, pp. 362–404.
6. Seitz, Frederick, and Read, T. A.: Theory of the Plastic Properties of Solids. I—Jour. Appl. Phys., vol. 12, no. 2, Feb. 1941, pp. 100–118; II—vol. 12, no. 3, March 1941, pp. 170–186; III—vol. 12, no. 6, June 1941, pp. 470–486; IV—vol. 12, no. 7, July 1941, pp. 538–554.
7. Kauzmann, Walter: Flow of Solid Metals from the Standpoint of the Chemical-Rate Theory. Trans. A. I. M. E., vol. 143, 1941, pp. 57–81.
8. Nowick, A. S., and Machlin, E. S.: Quantitative Treatment of the Creep of Metals by Dislocation and Rate-Process Theories. NACA Rep. 845, 1946.
9. Barrett, Charles Sanborn: Structure of Metals. McGraw-Hill Book Co., Inc., 1943, pp. 334–348.
10. Donnell, L. H.: Stress Concentrations due to Elliptical Discontinuities in Plates under Edge Forces. Theodore von Kármán Anniversary Volume, 1941, pp. 293–309.
11. Moore, Herbert F., and Ver, Tibor: A Study of Slip Lines, Strain Lines, and Cracks in Metals under Repeated Stress. Bull. No. 208, sec. 12, Univ. Ill., Eng. Exp. Sta., June 1930.
12. Gough, H. J., and Sopwith, D. G.: Some Further Experiments on Atmospheric Action in Fatigue. Jour. Inst. Metals, vol. LVI, no. 1, 1935, pp. 55–80; discussion, pp. 80–85; correspondence, pp. 85–89.
13. Gough, H. J.: Note on Some Fatigue and Density Tests Made of Aluminum Aggregate. R. & M. No. 1110, British A. R. C., 1928.
14. Gough, H. J., and Cox, H. L.: Mode of Deformation of a Single Crystal of Silver. R. & M. No. 1385, British A. R. C., 1931.
15. Irwin, P. L.: Fatigue of Metals by Direct Stress. Proc. A. S. T. M., vol. 26, pt. II, 1926, pp. 218–223.
16. Tapsell, H. J., and Clenshaw, W. J.: Properties of Materials at High Temperatures. Special Reps. Nos. 1 and 2, Dep't Sci. and Ind. Res., Eng. Res. (British), 1927.
17. Hankins, G. A.: Preliminary Report on the Properties of Commercially Pure Nickel as a Standard Material for Fatigue Investigations. R. & M. No. 789, British A. R. C., 1921.
18. Hopkinson, Bertram: A High-Speed Fatigue Tester, and the Endurance of Metals under Alternating Stresses of High Frequency. Proc. Roy. Soc. (London), ser. A, vol. 86, no. A 584, Jan. 31, 1912, pp. 131–149.
19. Stanton, Thomas Ernest, and Bairstow, Leonard: On the Resistance of Iron and Steel to Reversals of Direct Stress. Proc. Inst. Civil Eng., vol. CLXVI, April 10, 1906, pp. 78–110; discussion, pp. 111–124; correspondence, pp. 124–134.
20. Battelle Memorial Institute: Prevention of Failure of Metals under Repeated Stress. John Wiley & Sons, Inc., 1941, p. 202.
21. Dushman, Saul, Dunbar, L. W., and Huthsteiner, H.: Creep of Metals. Jour. Appl. Phys., vol. 15, no. 2, Feb. 1944, pp. 108–124.
22. Davis, Evan A.: Creep and Relaxation of Oxygen-Free Copper. Jour. Appl. Mech., vol. 10, no. 2, June 1943, pp. A101–A105.
23. Burghoff, H. L., and Blank, A. I.: Creep Characteristics of a Phosphorized Copper. Trans. A. I. M. E., Inst. Metals Div., vol. 161, 1945, pp. 420–440.
24. Michel, André, and Cournot, Jean: Contribution à l'Étude de la Viscosité à Chaud. Application à Divers Métaux et Alliages. Congrès International pour l'Essai des Matériaux (Amsterdam), t. I., Sept. 12–17, 1927, pp. 397–430.
25. Anon.: Compilation of Available High-Temperature Creep Characteristics of Metals and Alloys. Section A—Wrought 0.10 to 0.20 Per Cent Carbon Steels. Creep Data Sec., Joint Research Comm. on Effect of Temperature on the Properties of Metals. A. S. T. M. and A. S. M. E., March 1938, p. 22.
26. Elam, C. F.: Distortion of Metal Crystals. Clarendon Press (Oxford), 1935, p. 40.
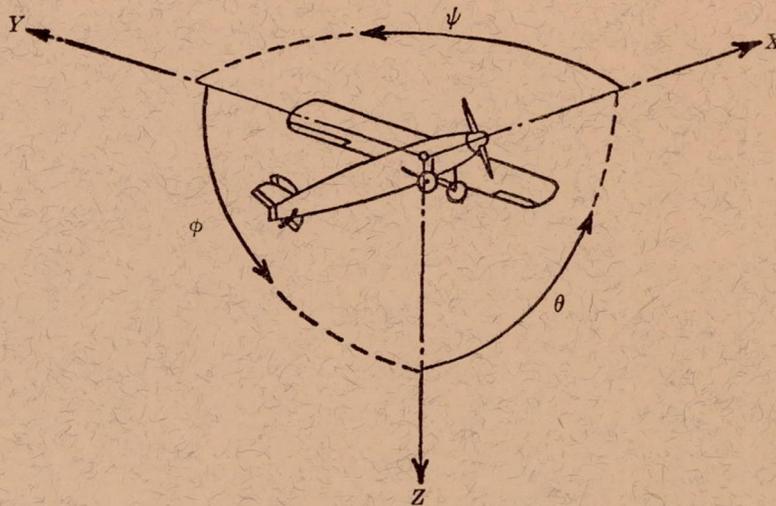
Positive directions of axes and angles (forces and moments) are shown by arrows

Axis		Force (parallel to axis) symbol	Moment about axis			Angle		Velocities	
Designation	Symbol		Designation	Symbol	Positive direction	Designation	Symbol	Linear (component along axis)	Angular
Longitudinal	X	X	Rolling	L	$Y \longrightarrow Z$	Roll	ϕ	u	p
Lateral	Y	Y	Pitching	M	$Z \longrightarrow X$	Pitch	θ	v	q
Normal	Z	Z	Yawing	N	$X \longrightarrow Y$	Yaw	ψ	w	r

Absolute coefficients of moment

$$C_l = \frac{L}{qbS} \qquad C_m = \frac{M}{qcS} \qquad C_n = \frac{N}{qbS}$$
$$\text{(rolling)} \qquad \text{(pitching)} \qquad \text{(yawing)}$$

Angle of set of control surface (relative to neutral position), δ. (Indicate surface by proper subscript.)

4. PROPELLER SYMBOLS

D Diameter

p Geometric pitch

p/D Pitch ratio

V' Inflow velocity

V_s Slipstream velocity

T Thrust, absolute coefficient $C_T = \dfrac{T}{\rho n^2 D^4}$

Q Torque, absolute coefficient $C_Q = \dfrac{Q}{\rho n^2 D^5}$

P Power, absolute coefficient $C_P = \dfrac{P}{\rho n^3 D^5}$

C_s Speed-power coefficient $= \sqrt[5]{\dfrac{\rho V^5}{P n^2}}$

η Efficiency

n Revolutions per second, rps

Φ Effective helix angle $= \tan^{-1}\left(\dfrac{V}{2\pi r n}\right)$

5. NUMERICAL RELATIONS

1 hp=76.04 kg-m/s=550 ft-lb/sec

1 metric horsepower=0.9863 hp

1 mph=0.4470 mps

1 mps=2.2369 mph

1 lb=0.4536 kg

1 kg=2.2046 lb

1 mi=1,609.35 m=5,280 ft

1 m=3.2808 ft